Journal of Fluorine Chemistry 129 (2008) 515–518

Contents lists available at ScienceDirect

Journal of Fluorine Chemistry

journal homepage: www.elsevier.com/locate/fluor

Preparation and optical properties of SrF_2:Eu^{3+} nanospheres

Ye Jin [a,b], Weiping Qin [c,*], Jisen Zhang [a]

[a] Key Laboratory of Excited State Processes, Changchun Institute of Optics, Fine Mechanics and Physics, Chinese Academy of Science, Changchun 130033, China
[b] Graduate School of Chinese Academy of Science, Beijing 100039, China
[c] State Key Laboratory of Integrated Optoelectronics, College of Electronic Science & Engineering, Jilin University, 2699 Qianjin Street, Changchun 130012, China

ARTICLE INFO

Article history:
Received 24 December 2007
Received in revised form 6 March 2008
Accepted 25 March 2008
Available online 30 March 2008

Keywords:
Morphology
SrF_2:Eu^{3+} nanospheres
Photoluminescence

ABSTRACT

SrF_2:Eu^{3+} nanospheres with homogeneous diameter have been synthesized by a microemulsion-mediated hydrothermal method for the first time, in which quaternary microemulsion of CTAB/water/cyclohexane/*n*-pentanol was used. The possible reaction mechanism and the luminescent properties of SrF_2:Eu^{3+} nanospheres were also investigated in this paper. The morphology and grain sizes of final products were characterized by field emission scanning electron microscopy and transmission electron microscopy, indicating that most of the products were nanospheres with an average diameter of ~50 nm. Room-temperature emission spectra, recorded under 394-nm excitation, showed that the transition of $^5D_0 \rightarrow {}^7F_1$ emission be dominating in SrF_2:Eu^{3+} nanospheres. From the dependence of the luminescence intensity on the concentration of Eu^{3+} ions, the optimal dopant concentration is 2 mol%.

1. Introduction

Fluorides have wide applications in optics as windows, lenses, scintillation crystals [1], and they are also as host crystals for rare earth ions (Ho, Er, Eu, Nd, Ce) exhibiting interesting properties in optoelectronics such as lasing [2], light amplification, and upconversion [3–5], alkaline-earth fluorides, such as CaF_2, SrF_2, and BaF_2 in cubic fluorite structure, constitute an important class of relatively simple ionic crystals, whose optical and lattice-dynamical properties are of much theoretical and experimental interest [6,7]. For instance, Falin et al. [8] reported optical spectroscopy of Yb^{3+} ions in CaF_2 and SrF_2. Bouffard et al. [4] showed red-to-blue upconversion spectroscopy of Tm^{3+} in SrF_2, CaF_2, BaF_2, and CdF_2.

Many efforts have generally focused on bulk alkaline-earth fluorides and other nanomaterials, such as carbon nanotubes, quantum dots, metallic nanoparticles, and metal oxide nanostructures, however, the preparation of low-dimensional alkaline-earth metal fluorides, including barium fluoride, strontium fluoride, and calcium fluoride, is at a nascent stage [9–15]. In 2000, Bender et al. [12] reported the synthesis of BaF_2:Nd^{3+} nanoparticles the reverse microemulsion technique. Three years later, Cao et al. [11] synthesized one-dimensional fluoride nanostructures—BaF_2 whiskers by a microemulsion-mediated hydrothermal method. Sun and Li [10] synthesized single crystal CaF_2 nanocubes by a simple hydrothermal method. Now, some workgroups have made some efforts on the synthesis of nanostructured EuF_3 [15] and other LnF_3 (Ln = La, Gd) [16–18], however, to the best of our knowledge no experimental study regarding on the homogeneous morphology strontium fluoride nanospheres has been reported up to now. In this letter, we have investigated the preparation of europium-ion-doped SrF_2 nanospheres and their photoluminescence properties.

2. Experimental

All the starting materials were of analytical grade and they were used as received from the supplier without further purification. In the experiment, a quaternary microemulsion, CTAB/water/cyclohexane/*n*-pentanol, was select. First, two identical transparent solutions were prepared by dissolving appropriate CTAB in a mixture of cyclohexane (6 mL) and *n*-pentanol (0.5 mL). A solution of $SrCl_2$ with $EuCl_3$ and a 40% HF solution (1 mL) were dropped into the solutions of CTAB, cyclohexane and *n*-pentanol, respectively, with vigorous stirring over 30 min at 30 °C. Thereafter, the two optically transparent microemulsion solutions were mixed together and the precursor microemulsion solution was obtained. It was transferred into a 25-mL stainless Teflon-lined autoclave subsequently and the autoclave was kept at 130 °C for 12 h. It was allowed to cool down to room temperature naturally, and the resulting suspension was stored at a constant temperature of 35 °C for 24 h. Following that, the product was collected and was washed several times with absolute ethanol and distilled water. Finally, the

* Corresponding author. Tel.: +86 431 85168240 8325; fax: +86 431 85168240 8325.
E-mail address: wpqin@jlu.edu.cn (W. Qin).

0022-1139/$ – see front matter © 2008 Elsevier B.V. All rights reserved.
doi:10.1016/j.jfluchem.2008.03.010

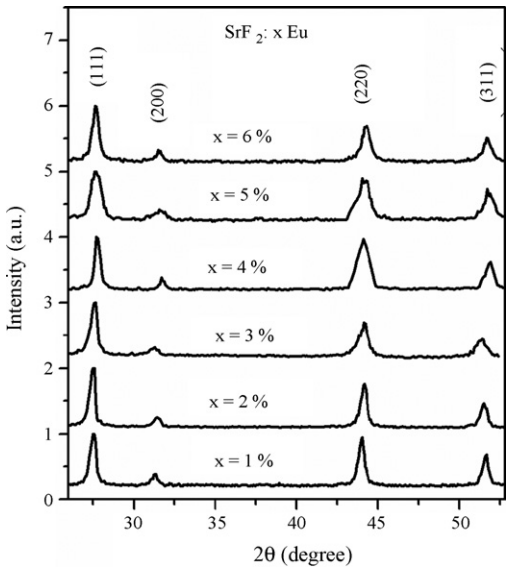

Fig. 1. XRD patterns of SrF_2 nanospheres with different Eu^{3+} concentrations.

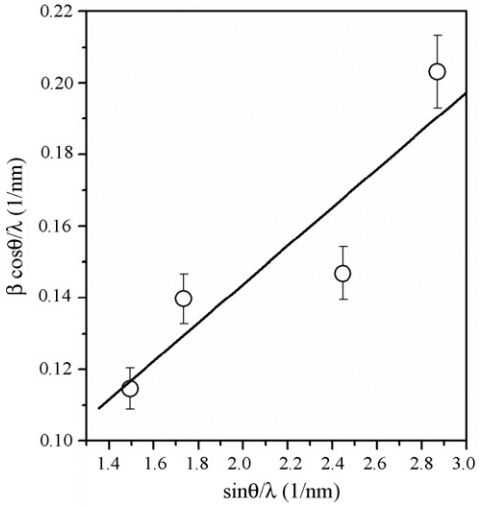

Fig. 2. Hall's plots of nanospheres SrF_2:3% Eu^{3+}.

result dispersion was centrifuged and dried in vacuum at room temperature. The white powder was obtained and the production quantity is about 0.4 mg SrF2 mL^{-1} reaction solution.

The structures of samples were characterized by X-ray diffraction (XRD) (Rigaku D/max-rA powder diffractometer with Cu target radiation resource (λ = 1.54078 Å)); the morphology and size were investigated by using field emission scanning electron microscopy (SEM) and transmission electron microscopy (TEM). Excitation and emission spectra were recorded at room temperature using a fluorescence spectrometer (Hitachi F-4500) with a 2.5-nm bandpass.

3. Results and discussion

The XRD patterns of SrF_2 nanospheres with different Eu^{3+} concentrations are shown in Fig. 1, and all of the diffraction peaks can be readily indexed to a pure cubic phase (space group: $Fm\bar{3}m$ (2 2 5)), which are in agreement with the standard values for cubic SrF_2 (JCPDS no. 86-2418) basically. No signals of Eu^{3+} were observed in the synthesized product owing to the low dopant concentration. The XRD results indicate that the products we obtained were SrF_2 nanoparticles. Hall's plots of SrF_2:3% Eu^{3+} as an example is shown in Fig. 2 and the lattice distortion can be obtained from the slope. For this sample, the distortion is 11.75% that is the biggest one in all of our products. When the concentrations of Eu^{3+} ions are 1 and 6%, the distortions are 2.3 and 1.4%, respectively. That is to say, here, the dopant concentration does not relate to the distortion.

Fig. 3 depicts that the morphology of the as-synthesized product is about 50-nm nanospheres. Fig. 3a is a wide-field SEM image of the as-prepared SrF_2:2% Eu^{3+} nanospheres, displaying that the products are composed of some homogeneous nanospheres with an average diameter about 50 nm. From SEM image of the sample, a distribution of nanospheric diameter was statistic, as shown in Fig. 4. The distribution of the nanospheric diameter is around 50 nm and the mean diameter is ~50.3 nm from Gaussian fit. Gaussian fit shows the clear tendency of diameter's distribution. More details about the product were investigated by TEM analysis (Fig. 3b) and the select area electronic diffraction (SAED) pattern (the inset). The sample for TEM characterization was prepared by placing a droplet of solution on a carbon-coated copper grid and letting it air-dry. TEM image shows the opaque nanosphere with clear outline on the copper grid. Moreover, the SEAD pattern displays SrF_2:Eu^{3+} is single crystal, which is taken from some single nanosphere. The energy-disperse X-ray (EDX) spectrum (see Fig. 5) taken from a single nanosphere further affirms the formation of SrF_2 phase and the percentage of Eu. The sample is SrF_2:5 mol% Eu^{3+} and the percentage of Eu^{3+} calculated by the computer is 2.56%.

In the experiment, CTAB is a surfactant in the water/oil microemulsion and the possible mechanism of the SrF_2:Eu^{3+} nanospherical formation is shown in Fig. 6. It was carried out

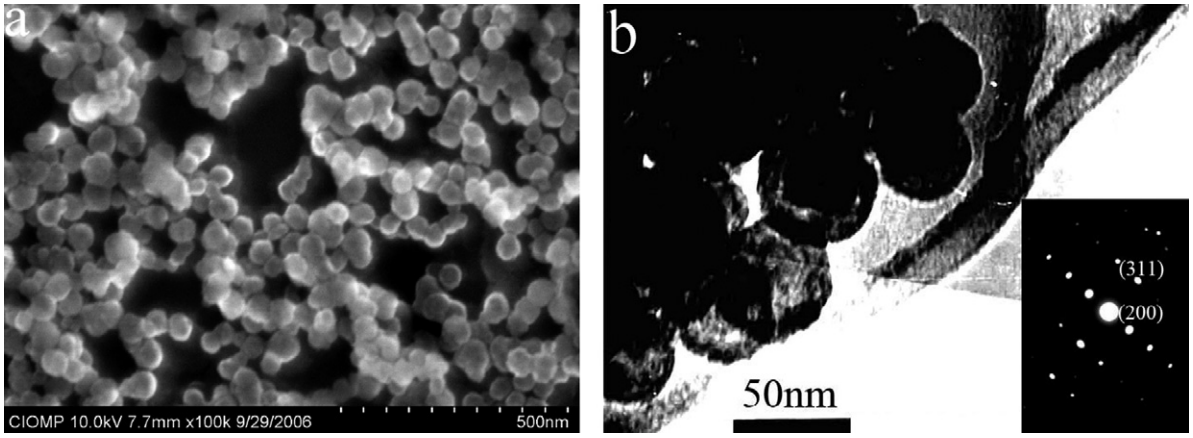

Fig. 3. (a) SEM image of SrF_2:Eu^{3+} nanospheres; (b) TEM image of SrF_2:Eu^{3+} nanospheres; inset: select area electron diffractions (SAEDs) recorded on individual nanospheres.

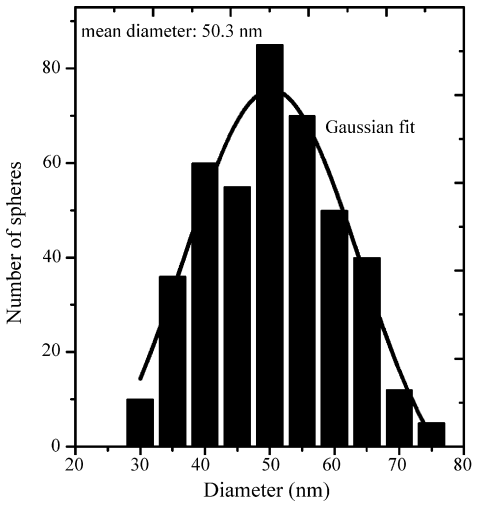

Fig. 4. Histogram of the particle size distribution obtained from SEM images (Fig. 2a).

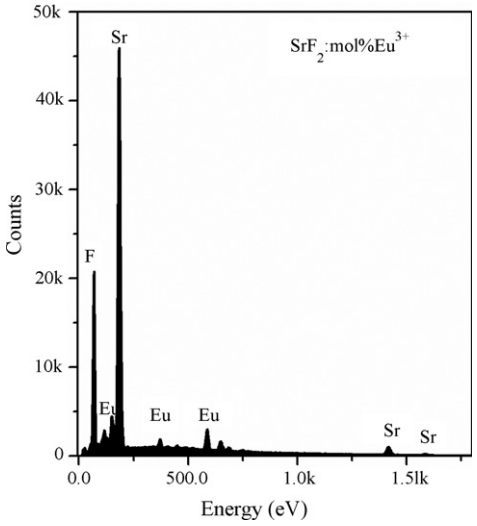

Fig. 5. Representative EDX spectrum of a single nanosphere of SrF_2:5 mol% Eu^{3+}.

through three steps as follows: (1) the formation of the microemulsion drop. The surfactant often has hydrophilic group and hydrophobic group. CTAB is solved in the mixed solution of cyclohexane and *n*-pentanol, and the microemulsion environment begins to been set up. (2) After the hydrophilic hydrophobic balance, the formation of precipitation of SrF_2:Eu^{3+} in the microemulsion drop. (3) The formation of SrF_2:Eu^{3+} nanospheres. The microemulsion drop is like a very small reaction vessel that limits the growing up of the particles.

Room-temperature emission spectra of SrF_2 with different Eu^{3+} concentrations have been investigated, which is shown in Fig. 7. Some emission lines have been observed in the emission spectrum,

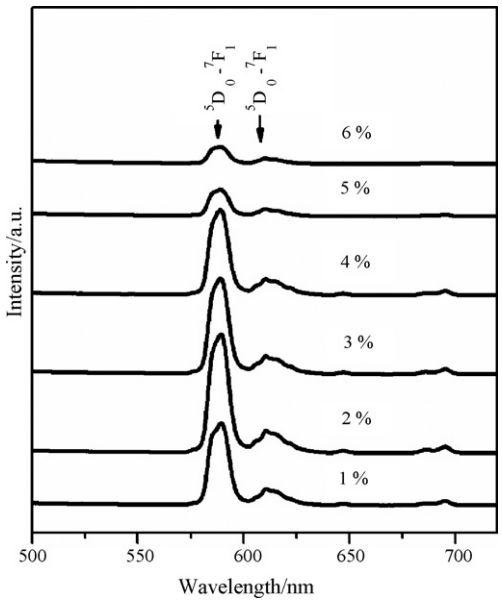

Fig. 7. Room-temperature emission spectra of SrF_2:Eu^{3+} nanospheres (λ_{ex} = 394 nm) with different Eu^{3+} concentrations.

which are associated with the transitions of Eu^{3+} ions from the $^5D_0$ level to ^7F_J (J = 0, 1, 2, 3, 4) levels. The emission of $^5D_0 \rightarrow {}^7F_0$ transition can be observed only when Eu^{3+} ions locate in low symmetric sites. The $^5D_0 \rightarrow {}^7F_1$ transition is parity-allowed magnetic dipole transition, which is slightly affected by the symmetry of the Eu^{3+} site. The $^5D_0 \rightarrow {}^7F_2$ transition is a parity-forbidden electric dipole transition and the probability of its transition is very sensitive to relatively small changes of the environment around Eu^{3+} ions. Its strong emission only occurs in non-inversion symmetry sites. So the Eu^{3+} ion is often occupied as a probe to detect the surroundings of the matrix. In the spectra, the $^5D_0 \rightarrow {}^7F_1$ transition is much stronger than others and the $^5D_0 \rightarrow {}^7F_0$, $^5D_0 \rightarrow {}^7F_3$, $^5D_0 \rightarrow {}^7F_4$ transitions are hardly observed. Moreover, the emission intensity is related to the dopant concentration of Eu^{3+} ions. In Fig. 8, it shows the dependence of the integrated luminescence intensity of SrF_2:Eu^{3+} nanospheres on the concentration of Eu^{3+} ion dopant by monitoring the emission of $^5D_0 \rightarrow {}^7F_1$ transition at 590 nm, which was calculated from Fig. 6. The luminescence intensity was enhanced with the increasing Eu^{3+} concentration when it lower than 2 mol% and it reached to the maximum at 2 mol% of Eu^{3+} ions. For higher Eu^{3+} concentration, there is a significant decrease of the luminescence intensity. So for Eu^{3+}-doped SrF_2, the quenching concentration is about 2 mol%. The decrease of the integrated luminescence intensity of SrF_2:Eu^{3+} on the concentration of Eu^{3+} ion dopant is affected by two main points. One is the distortion of the lattice caused by the high doping; the other is energy dispersion between Eu^{3+} ions. The effect of the distortion of the lattice caused by the high doping to the luminescence has been excluded in the forgoing Fig. 2. The concentration quenching should be attributed to the non-radiative

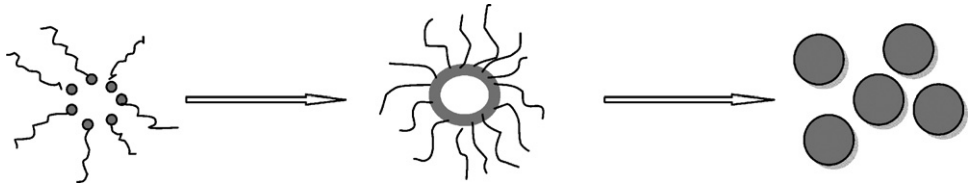

Fig. 6. A schematic diagram of the formation mechanism of the spherical SrF_2:Eu^{3+} nanocrystal.

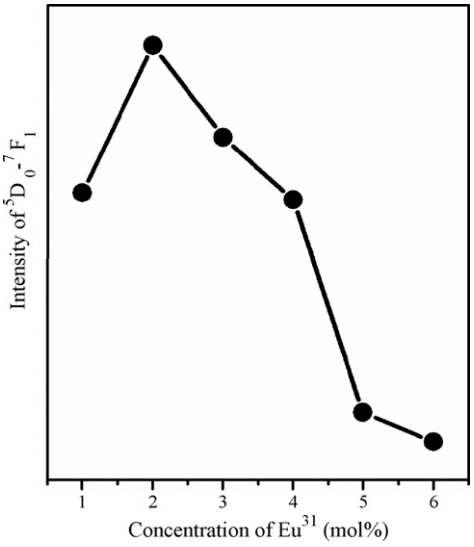

Fig. 8. Luminescent intensity of SrF_2:Eu^{3+} depending on Eu^{3+} concentration.

transfer resulted from resonance energy transfer between adjacent europium (III) ions which was publicly studied by the researchers [19,20].

The quantum yield of SrF_2:2 mol% Eu^{3+} is 2.5%. PL quantum yields of SrF_2:Eu^{3+} ethanol solution were measured by comparing the integrated emission of an ethanol solution of Rhodamin 6G (laser grade; quantum yield 95%) under 394-nm excitation.

4. Conclusions

In conclusion, the current report describes the synthesis of pure phase SrF_2:Eu^{3+} nanospheres in uniform diameter of ~50 nm by quaternary microemulsion-mediated hydrothermal method. It is noteworthy that the quaternary microemulsion-mediated hydrothermal method is effective for obtained pure phase nanomaterials with controllable size, uniform morphology and shape. Resulting nanospheres have been characterized using spectroscopy data. From the dependence of the luminescence intensity on the concentration of Eu^{3+}, the optimal concentration of dopant Eu^{3+} ions for SrF_2 nanosphere was about 2 mol%. The synthesis and the luminescence properties of SrF_2:Eu^{3+} nanospheres provide a basis for our more thorough investigation of further optical and optoelectronic properties into nanoscale devices.

Acknowledgements

The authors gratefully acknowledge financial support for this research from the National Natural Science Foundation of China (grant nos. are 10474096 and 50672030).

References

[1] E. Slunga, B. Cederwall, E. Ideguchi, A. Kerek, W. Klamra, J. van der Marel, D. Novak, L.-O. Norlin, Nucl. Instrum. Methods Phys. Res. Sect. A 469 (2001) 70–76.
[2] T.T. Basiev, et al. Laser Phys. 12 (2002) 859–877.
[3] P. Goldner, M. Mortier, J. Non-Cryst. Solids 284 (2001) 249–254.
[4] M. Bouffard, J.P. Jouart, M.F. Joubert, Opt. Mater. 14 (2000) 73–79.
[5] X. Zhang, X.R. Liu, J.P. Jouart, G. Mary, Chem. Phys. Lett. 287 (1998) 659–662.
[6] G.A. Samara, Phys. Rev. B 13 (1976) 4529–4544.
[7] R.M. Hazen, L.W. Finger, J. Appl. Cryst. 14 (1981) 234–236.
[8] M.L. Falin, K.I. Gerasimov, V.A. Latypov, A.M. Leushin, H. Bill, D. Lovy, J. Lumin. 102/103 (2003) 239–242.
[9] F. Wang, X. Fan, D. Pi, M. Wang, Solid State Commun. 133 (2005) 775–779.
[10] X. Sun, Y. Li, Chem. Commun. 14 (2003) 1768–1769.
[11] M. Cao, C. Hu, E. Wang, J. Am. Chem. Soc. 125 (2003) 11196–11197.
[12] C.M. Bender, J.M. Burlitch, D. Barber, C. Pollock, Chem. Mater. 12 (2000) 1969–1976.
[13] R.N. Grass, W.J. Stark, Chem. Commun. 13 (2005) 1767–1769.
[14] Y. Mao, F. Zhang, S.S. Wong, Adv. Mater. 18 (2006) 1895–1899.
[15] M. Wang, Q.L. Huang, J.M. Hong, X.T. Chen, Z.L. Xue, Cryst. Growth Des. 6 (2006) 2169–2173.
[16] F. Evanics, P.R. Diamente, F.C.J.M. van Veggel, G.J. Stanisz, R.S. Prosser, Chem. Mater. 18 (2006) 2499–2505.
[17] Y.W. Zhang, X. Sun, R. Si, L.P. You, C.H. Yan, J. Am. Chem. Soc. 127 (2005) 3260–3261.
[18] J.W. Stouwdam, F.C.J.M. van Veggel, Nano Lett. 2 (2002) 733–737.
[19] G. Blasse, J. Lumin. 1/2 (1970) 766–777.
[20] Z.K. Wei, L.D. Sun, C.S. Liao, C.H. Yan, S.H. Huang, Appl. Phys. Lett. 80 (2002) 1447–1449.